

Syracuse University

**SURFACE**

---

Physics

College of Arts and Sciences

---

3-7-2012

## Electron drift-mobility measurements in polycrystalline CuIn<sub>1-x</sub>Ga<sub>x</sub>Se<sub>2</sub> solar cells

Steluta A. Dinca  
*Syracuse University*

Eric A. Schiff  
*Syracuse University*


William N. Shafarman  
*University of Delaware*

Brian Egaas  
*National Renewable Energy Laboratory*

Rommel Noufi  
*National Renewable Energy Laboratory*

*See next page for additional authors*

Follow this and additional works at: <https://surface.syr.edu/phy>

 Part of the [Condensed Matter Physics Commons](#), and the [Electronic Devices and Semiconductor Manufacturing Commons](#)

---

### Recommended Citation

Dinca, Steluta A.; Schiff, Eric A.; Shafarman, William N.; Egaas, Brian; Noufi, Rommel; and Young, David L., "Electron drift-mobility measurements in polycrystalline CuIn<sub>1-x</sub>Ga<sub>x</sub>Se<sub>2</sub> solar cells" (2012). *Physics*. 515. <https://surface.syr.edu/phy/515>

This Article is brought to you for free and open access by the College of Arts and Sciences at SURFACE. It has been accepted for inclusion in Physics by an authorized administrator of SURFACE. For more information, please contact [surface@syr.edu](mailto:surface@syr.edu).

---

**Authors/Contributors**

Steluta A. Dinca, Eric A. Schiff, William N. Shafarman, Brian Egaas, Rommel Noufi, and David L. Young

## Electron drift-mobility measurements in polycrystalline $\text{CuIn}_{1-x}\text{Ga}_x\text{Se}_2$ solar cells

S. A. Dinca, E. A. Schiff, W. N. Shafarman, B. Egaas, R. Noufi et al.

Citation: *Appl. Phys. Lett.* **100**, 103901 (2012); doi: 10.1063/1.3692165

View online: <http://dx.doi.org/10.1063/1.3692165>

View Table of Contents: <http://apl.aip.org/resource/1/APPLAB/v100/i10>

Published by the [American Institute of Physics](#).

---

### Related Articles

Modeling metastabilities in chalcopyrite-based thin film solar cells

*J. Appl. Phys.* **111**, 043703 (2012)

Crystal and electronic structures of  $\text{Cu}_x\text{S}$  solar cell absorbers

*Appl. Phys. Lett.* **100**, 061906 (2012)

Electrical modeling of  $\text{Cu}(\text{In,Ga})\text{Se}_2$  cells with ALD- $\text{Zn}_{1-x}\text{Mg}_x\text{O}$  buffer layers

*J. Appl. Phys.* **111**, 014509 (2012)

Determination of secondary phases in kesterite  $\text{Cu}_2\text{ZnSnS}_4$  thin films by x-ray absorption near edge structure analysis

*Appl. Phys. Lett.* **99**, 262105 (2011)

Comparative atom probe study of  $\text{Cu}(\text{In,Ga})\text{Se}_2$  thin-film solar cells deposited on soda-lime glass and mild steel substrates

*J. Appl. Phys.* **110**, 124513 (2011)

---

### Additional information on *Appl. Phys. Lett.*

Journal Homepage: <http://apl.aip.org/>

Journal Information: [http://apl.aip.org/about/about\\_the\\_journal](http://apl.aip.org/about/about_the_journal)

Top downloads: [http://apl.aip.org/features/most\\_downloaded](http://apl.aip.org/features/most_downloaded)

Information for Authors: <http://apl.aip.org/authors>

## ADVERTISEMENT

**NEW!**

**iPeerReview**  
AIP's Newest App



**Authors...  
Reviewers...  
Click the status of  
submitted papers remotely!**

**AIP** | Publishing

## Electron drift-mobility measurements in polycrystalline $\text{CuIn}_{1-x}\text{Ga}_x\text{Se}_2$ solar cells

S. A. Dinca,<sup>1,a)</sup> E. A. Schiff,<sup>1</sup> W. N. Shafarman,<sup>2</sup> B. Egaas,<sup>3</sup> R. Noufi,<sup>3</sup> and D. L. Young<sup>3</sup>

<sup>1</sup>Department of Physics, Syracuse University, Syracuse, New York 13244-1130, USA

<sup>2</sup>Institute of Energy Conversion, University of Delaware, Newark, Delaware 19716, USA

<sup>3</sup>National Renewable Energy Laboratory, Golden, Colorado 80401, USA

(Received 21 September 2011; accepted 10 February 2012; published online 7 March 2012)

We report photocarrier time-of-flight measurements of electron drift mobilities for the  $p$ -type  $\text{CuIn}_{1-x}\text{Ga}_x\text{Se}_2$  films incorporated in solar cells. The electron mobilities range from 0.02 to 0.05  $\text{cm}^2/\text{Vs}$  and are weakly temperature-dependent from 100–300 K. These values are lower than the range of electron Hall mobilities (2–1100  $\text{cm}^2/\text{Vs}$ ) reported for  $n$ -type polycrystalline thin films and single crystals. We propose that the electron drift mobilities are properties of disorder-induced mobility edges and discuss how this disorder could increase cell efficiencies. © 2012 American Institute of Physics. [<http://dx.doi.org/10.1063/1.3692165>]

The chalcopyrite alloys  $\text{CuIn}_{1-x}\text{Ga}_x\text{Se}_2$  (CIGS) are the basis of very promising thin film solar cells, with solar conversion efficiencies up to 20.3%.<sup>1</sup> Despite the remarkable efficiencies, fundamental properties such as the minority carrier (electron) mobility are not established for the materials used in cells, and their device physics has necessarily been based on informed parameter guesses.<sup>2,3</sup>

In this letter, we present photocarrier time-of-flight (TOF) measurements of electron drift-mobilities in  $p$ -type CIGS thin films incorporated into solar cells. In samples from the Institute of Energy Conversion (IEC) and from the National Renewable Energy Laboratory (NREL), we find electron mobilities in the range 0.02–0.05  $\text{cm}^2/\text{Vs}$ . These are lower than the Hall mobilities of electrons in  $n$ -type CIGS materials, which range from 2–1100  $\text{cm}^2/\text{Vs}$ .<sup>4–6</sup> They are also lower than the electron drift mobility<sup>7</sup> reported for a single crystal of  $p$ -type  $\text{CuInSe}_2$  and are nearly  $10^3$  smaller than the band mobility assumed in some device models. The magnitude of the electron drift mobilities is consistent with disorder-induced mobility-edges dividing localized and delocalized conduction band states.<sup>8,9</sup> Empirical optimization of CIGS for solar cells thus appears to have led to low-mobility materials. We speculate that the disorder that lowers the mobilities also improves the optical absorption in the films, presumably by weakening the optical selection rules. The values of the electron mobilities that we measure are also self-consistent with the typical thickness and with the use of  $n$ -type CdS top contacts for thin-film CIGS solar cells.

We studied four polycrystalline CIGS solar cells. The cells were grown on Mo-coated soda-lime glass substrates in the sequence: glass/Mo/ $\text{CuIn}_{1-x}\text{Ga}_x\text{Se}_2$ /CdS/ZnO. The CIGS cell from NREL was deposited under high vacuum conditions by coevaporation from elemental sources following the “three-stage” process.<sup>10</sup> The cells from IEC were grown using single-stage four source elemental evaporation.<sup>11</sup> The CIGS layers had an alloy ratio  $[\text{Ga}]/([\text{In}] + [\text{Ga}])$  of about

0.3 and were  $p$ -type. The photovoltaic parameters of the specimens used in this research are summarized in Table I.

Conventional electron TOF measurements on CIGS solar cells would use strongly absorbed light pulses incident through the back of the cell, which was not possible with our Mo-coated substrates. We used an extension of the TOF technique with uniformly absorbed illumination incident through the front, which requires an analysis to separate the electron and hole contributions to the transient photocurrent. The method is not common, but has been used previously.<sup>12,13</sup>

Transient photocurrent measurements were performed using a short flash of light from single mode laser diodes. The CIGS devices were illuminated through the top,  $n$ -type CdS buffer layer. The TOF experiments were done at two wavelengths, 690 and 1050 nm, with a typical photon flux around  $10^9 \text{ cm}^{-2}$ . The 690 nm light is absorbed in the CIGS film within about 100 nm from the CdS buffer, and the 1050 nm light is absorbed uniformly throughout the CIGS film.<sup>14</sup> We used DC voltage bias. The transient photocurrent responses to the laser pulses were recorded, averaged, and integrated to obtain the transient photocharge.

In Figure 1, we present the transient photocharge  $Q(t)$  at 150 K with a reverse bias voltage of  $-0.1 \text{ V}$  on an IEC sample. We chose this sample and temperature to illustrate the experiment because the width of the “depletion layer”

TABLE I. Properties of the  $\text{CuIn}_{1-x}\text{Cu}_x\text{Se}_2$  specimens used in the TOF measurements at 293 K.  $V_{OC}$  is the open circuit voltage,  $J_{SC}$  is the short circuit current,  $L$  is the geometrical thickness,  $d$  is the width of the depletion layer at 0 V, and  $\mu_h$  and  $\mu_e$  are the hole and electron drift-mobilities.

Sample	NREL	IEC
$V_{OC}$ (V)	0.63	0.62
$J_{SC}$ ( $\text{mA}/\text{cm}^2$ )	30.9	33.4
Efficiency (%)	13.3	15.0
$L$ ( $\mu\text{m}$ )	2.6	2.0
$d$ ( $\mu\text{m}$ )	1.1	0.7
$\mu_h$ ( $\text{cm}^2/\text{Vs}$ )	0.4	0.1–0.5
$\mu_e$ ( $\text{cm}^2/\text{Vs}$ )	0.05	0.02–0.03

<sup>a)</sup>Author to whom correspondence should be addressed. Electronic mail: [sdinca@phy.syr.edu](mailto:sdinca@phy.syr.edu).

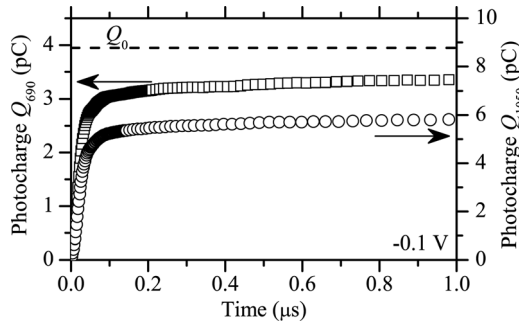


FIG. 1. Transient photocharge  $Q(t)$  measured at 690 nm and 1050 nm in a CIGS sample IEC at 150 K with a reversed bias voltage of  $-0.1$  V. Fiduciary line  $Q_0$  represents the total mobile charges generated in the specimen by the two laser impulses.

inferred from capacitance had a weak voltage-dependence, indicating a nearly uniform electric field. While convenient, this behavior was unusual, and we do not have a simple model for it. At room-temperature, the depletion layer width increased with reverse bias voltage for all samples, as anticipated from Schottky and related analyses. The measurements and analysis for these conditions are presented as supplementary materials.<sup>6</sup>

For the 690 nm transient, the rapid rise in the photocharge over the first 50 ns corresponds primarily to holes drifting deeper into the CIGS film. The dashed line indicates the value of the total photogenerated charge  $Q_0$  inferred from measurements at larger reverse bias; the long-time value for  $Q(t)$  does not reach  $Q_0$  for this voltage because of “deep trapping” by defects. We have previously reported similar hole drift-mobility measurements.<sup>15</sup>

For the 1050 nm illumination, both electron and hole photocarriers contribute equally to the total photocharge  $Q_0$ . The initial rise of the photocharge is somewhat slower than for 690 nm, which reflects a slower drift of electrons compared to holes. At longer times, the charge collection is also not as complete as for 690 nm, which reflects stronger trapping of the electrons than the holes.

In Figure 2, we present our analysis of the voltage-dependent photocharge. The symbols indicate the photocharge  $Q$  measured at  $4 \mu\text{s}$ ; photocharge collection was complete by this time. The lines passing near the symbols are

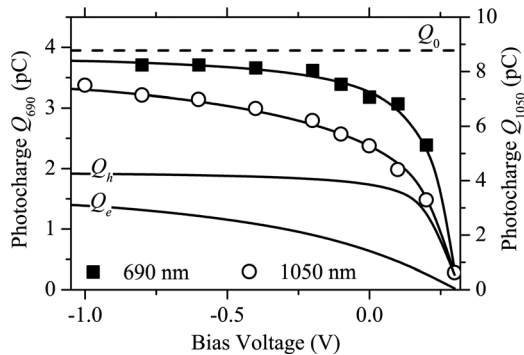


FIG. 2. The symbols indicate the photocharge  $Q$  measured at  $4 \mu\text{s}$  for varying bias voltages on sample IEC; results for two optical wavelengths are shown. The solid lines through data are fittings using the Hecht equations (Ref. 15). The curves,  $Q_e$  and  $Q_h$ , are calculations of the electron and hole contributions at 1050 nm ( $\mu\tau_h = 8.3 \times 10^{-8} \text{ cm}^2/\text{V}$ ,  $\mu\tau_e = 6.5 \times 10^{-9} \text{ cm}^2/\text{V}$ , and  $V_0 = 0.31 \text{ V}$ ).

fittings to expressions involving  $Q_0$ , an offset-voltage  $V_0$ , and electron and hole deep-trapping mobility-lifetime products  $\mu\tau_h$  and  $\mu\tau_e$ , respectively. The 690 nm photocharge shows a clear saturation near  $-1$  V; this means that holes were able to traverse the depletion layer without being trapped. The fitting to the standard Hecht equation<sup>15</sup> yielded  $\mu\tau_h = 8.3 \times 10^{-8} \text{ cm}^2/\text{V}$  and  $V_0 = 0.31 \text{ V}$ .  $V_0$  is lower than the built-in potential  $V_{BI}$ , which we think reflects a rapid drop of the built-in electric potential near the CIGS/CdS interface.<sup>15</sup>

For 1050 nm illumination, holes and electrons are uniformly photogenerated. The expression for the charge collection is given as Eq. (B10) in the supplementary material.<sup>6</sup> The curve uses the values  $\mu\tau_h$  and  $V_0$  from the 690 nm measurement and also  $\mu\tau_e$ , which is a fitting parameter. We obtained  $\mu\tau_e = 6.5 \times 10^{-9} \text{ cm}^2/\text{V}$ , which is about ten times smaller than the hole deep-trapping parameter  $\mu\tau_h$ .

To obtain the drift mobilities, we analyzed the full transient photocharge  $Q(t)$  using 1050 nm illumination, as illustrated in Fig. 3. The hole mobility  $\mu_h = 0.6 \text{ cm}^2/\text{Vs}$  had been determined from the 690 nm measurements using standard procedures,<sup>15</sup> so only the electron mobility  $\mu_e$  was unknown. The measured photocharge is the sum of the electron and hole components  $Q_e(t)$  and  $Q_h(t)$

$$Q(t) = Q_e(t) + Q_h(t). \quad (1)$$

The expression for the transient photocharge  $Q(t)$  is provided in Eq. (B8) of the supplementary materials.<sup>6</sup> We obtained

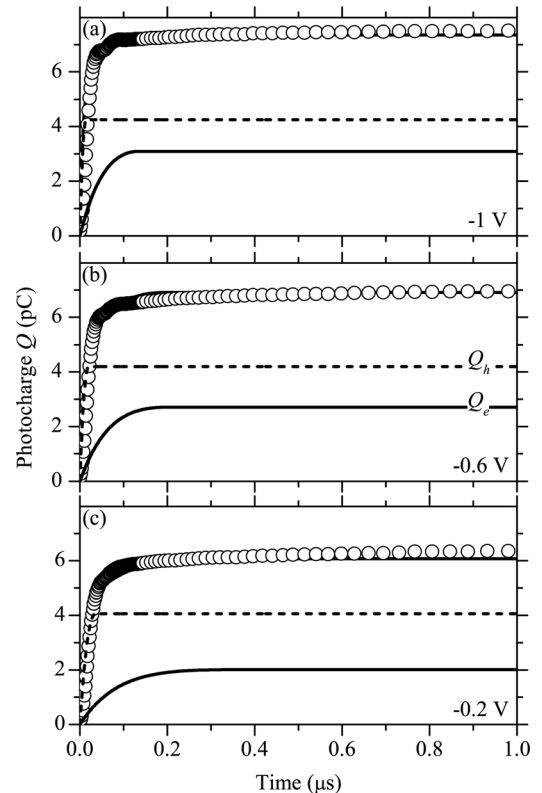


FIG. 3. Transient photocharge  $Q(t)$  at varying bias voltages in a specimen (IEC) at  $T = 150 \text{ K}$ . Symbols indicate measurements at 1050 nm. The curves through these data are fittings using Eq. (1). The dashed lines indicate the hole transient photocharge,  $Q_h$ . The solid lines are the electron transient photocharge,  $Q_e$ . ( $\mu_h = 0.6 \text{ cm}^2/\text{Vs}$  and  $\mu_e = 0.06 \text{ cm}^2/\text{Vs}$ ).

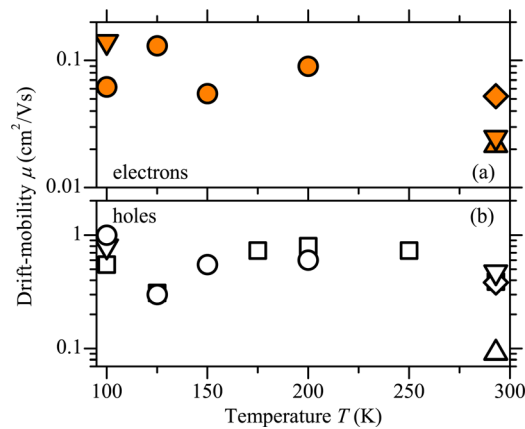


FIG. 4. (Color online) Electron and hole drift-mobility  $\mu$  measurements as a function of temperature in polycrystalline CIGS. Symbol shape indicates a particular cell. References are: —, X—IEC (different cells); M—NREL; and □—IEC-2 (Ref. 15).

$\mu_e = 0.06 \text{ cm}^2/\text{Vs}$  by fitting these transients and several others that are not shown; as can be seen in Fig. 3, the corresponding calculations are reasonably consistent with the measurements.

We applied these procedures at several temperatures and to several samples. The main additional complication that did not arise for the measurements of Figs. 1–3 was voltage-dependent widths for the depletion layer. We have previously reported our procedures for analyzing TOF measurements in this circumstance.<sup>15</sup> In Fig. 4, we summarize our temperature-dependent findings for electrons and holes mobility in several samples; some of the hole measurements are from our previous paper using comparable samples.<sup>15,16</sup> We summarize the room-temperature parameters in Table I.

For the IEC cell, our 150 K estimate of electron deep-trapping mobility-lifetime product  $\mu\tau_e = 7 \times 10^{-9} \text{ cm}^2/\text{V}$  is somewhat larger than the value  $2 \times 10^{-9} \text{ cm}^2/\text{V}$  reported by Heath *et al.*<sup>17</sup> For the NREL cells, our room-temperature  $\mu\tau_e = 2.5 \times 10^{-7} \text{ cm}^2/\text{V}$  value is consistent with recent diffusion length measurements.<sup>18</sup>

The magnitude  $\mu_e < 1 \text{ cm}^2/\text{Vs}$  suggests that this mobility is associated with disorder induced formation of a mobility edge dividing localized and delocalized states near the bandedges, which is well known in some amorphous and nanocrystalline semiconductors.<sup>9</sup> We think that it is plausible that the electron mobilities are reduced by the previously reported nanometer-scale chemical composition fluctuations in materials similar to ours,<sup>19</sup> and several investigators have speculated on the role of disorder on the optoelectronic properties of CIGS.<sup>20</sup> It is remarkable that these electron mobilities, which are properties of materials similar to those that have yielded very high solar cell efficiencies, are lower than the Hall mobilities previously reported for *n*-type films, which ranged from 2–1100  $\text{cm}^2/\text{Vs}$ .<sup>6</sup> We speculate that the empirical optimization of CIGS solar cells at a given electri-

cal bandgap has traded off disorder-induced diminishment of carrier mobilities for disorder-induced increase in optical absorption.

The electron mobilities are lower than the hole mobilities in our cells. This result is consistent with the design of CIGS cells, which places an *n*-type contact (CdS) as a window layer in the cells so that electrons are photogenerated as close as possible to their collecting contact. The magnitude of the electron mobility also affects the width of the space-charge region near the top contact. The region's width  $L_{sc}$  under illumination is at most  $L_{sc} \approx ((2/3)V_{OC})^{1/2} (\mu_e \epsilon \epsilon_0 / eG)^{1/4}$ , where  $G \approx J_{sc}/Le \approx 10^{21} \text{ cm}^{-3} \text{ s}^{-1}$  is the average photogeneration rate (cf. Table I),  $\epsilon \epsilon_0$  is the dielectric constant, and  $e$  the electronic charge.<sup>21</sup> For  $\mu_e \approx 0.1 \text{ cm}^2/\text{Vs}$ , we estimate  $L_{sc} \approx 0.9 \mu\text{m}$ .

<sup>1</sup>M. A. Green, K. Emery, Y. Hishikawa, and W. Warta, *Prog. Photovoltaics* **19**, 84 (2011).

<sup>2</sup>M. Gloeckler and J. R. Sites, *Thin Solid Films* **480–481**, 241 (2005).

<sup>3</sup>J. Song, T. J. Anderson, and S. S. Li, in *Proceedings of 33rd IEEE Photovoltaic Specialists Conference, San Diego, CA* (IEEE, Piscataway, 2008), p. 1.

<sup>4</sup>B. Schumann, H. Neumann, A. Tempel, G. Kühn, and E. Nowak, *Cryst. Res. Technol.* **15**, 71 (1980).

<sup>5</sup>S. M. Firoz Hasan, M. A. Subhan, and Kh. M. Mannan, *Opt. Mater.* **14**, 329 (2000).

<sup>6</sup>See supplementary material at <http://dx.doi.org/10.1063/1.3692165> for references to electron Hall mobilities in *n*-type CIGS materials, measurements and analysis with voltage-dependent depletion widths, and the photocurrent and photocharge expressions.

<sup>7</sup>M. Tabib-Azar, H.-J. Moller, and N. Shoemaker, *IEEE Trans. Ultrason. Ferroelectr. Freq. Control* **40**, 149 (1993).

<sup>8</sup>N. F. Mott, *Conduction in Non-Crystalline Materials*, 2nd ed. (Oxford University Press, Oxford, 1993).

<sup>9</sup>E. A. Schiff, *J. Phys.: Condens. Matter* **16**, S5265 (2004).

<sup>10</sup>I. Repins, M. A. Contreras, B. Egaas, C. DeHart, J. Scharf, C. L. Perkins, B. To, and R. Noufi, *Prog. Photovoltaics* **16**, 235 (2008).

<sup>11</sup>W. N. Shafarman, R. Klenk, and B. E. McCandless, *J. Appl. Phys.* **79**, 9 (1996).

<sup>12</sup>S. A. Dinca, E. A. Schiff, S. Guha, B. Yan, and J. Yang, *Mater. Res. Soc. Symp. Proc.* **1153**, A16-07 (2009).

<sup>13</sup>R. A. Street, K. W. Song, J. E. Northrup, and S. Cowan, *Phys. Rev. B* **83**, 165207 (2011).

<sup>14</sup>M. I. Alonso, M. Garriga, C. A. D. Rinçon, E. Hernández, and M. León, *Appl. Phys. A* **74**, 659 (2002).

<sup>15</sup>S. A. Dinca, E. A. Schiff, B. Egaas, R. Noufi, D. L. Young, and W. N. Shafarman, *Phys. Rev. B* **80**, 235201 (2009).

<sup>16</sup>Some electron mobilities were estimated using only the 1050 nm measurements; we found results with this procedure to be consistent with the more extensive one that we described above that used both 690 nm and 1050 nm measurements.

<sup>17</sup>J. T. Heath, J. D. Cohen, W. N. Shafarman, D. X. Liao, and A. A. Rockett, *Appl. Phys. Lett.* **80**, 4540 (2002).

<sup>18</sup>G. Brown, V. Faifer, A. Pudov, S. Anikeev, E. Bykov, M. Contreras, and J. Wu, *Appl. Phys. Lett.* **96**, 022104 (2010). Assuming electron deep-trapping is the recombination event, we obtain the ambipolar diffusion length for  $L_{amb} \approx ((kT/e)\mu\tau_e)^{1/2}$ ; for  $\mu\tau_e = 10^{-7} \text{ cm}^2/\text{V}$  and  $L_{amb} = 0.5 \mu\text{m}$ , which is consistent with this reference.

<sup>19</sup>Y. Yan, R. Noufi, K. M. Jones, K. Ramanathan, M. M. Al-Jassim, and B. J. Stanbery, *Appl. Phys. Lett.* **87**, 121904 (2005).

<sup>20</sup>J. H. Werner, J. Mattheis, and U. Rau, *Thin Solid Films* **480–481**, 399 (2005).

<sup>21</sup>E. A. Schiff, *Sol. Energy Mater. Sol. Cells* **78**, 567 (2003).